



This is a repository copy of *Technical performance analysis and economic evaluation of a compressed air energy storage system integrated with an organic Rankine cycle*.

White Rose Research Online URL for this paper:  
<http://eprints.whiterose.ac.uk/121906/>

Version: Accepted Version

---

**Article:**

Meng, H., Wang, M. [orcid.org/0000-0001-9752-270X](https://orcid.org/0000-0001-9752-270X), Aneke, M. et al. (3 more authors) (2018) Technical performance analysis and economic evaluation of a compressed air energy storage system integrated with an organic Rankine cycle. *Fuel*, 211. pp. 318-330. ISSN 0016-2361

<https://doi.org/10.1016/j.fuel.2017.09.042>

---

Article available under the terms of the CC-BY-NC-ND licence (<https://creativecommons.org/licenses/by-nc-nd/4.0/>).

**Reuse**

This article is distributed under the terms of the Creative Commons Attribution-NonCommercial-NoDerivs (CC BY-NC-ND) licence. This licence only allows you to download this work and share it with others as long as you credit the authors, but you can't change the article in any way or use it commercially. More information and the full terms of the licence here: <https://creativecommons.org/licenses/>

**Takedown**

If you consider content in White Rose Research Online to be in breach of UK law, please notify us by emailing [eprints@whiterose.ac.uk](mailto:eprints@whiterose.ac.uk) including the URL of the record and the reason for the withdrawal request.



[eprints@whiterose.ac.uk](mailto:eprints@whiterose.ac.uk)  
<https://eprints.whiterose.ac.uk/>

# Technical performance analysis and economic evaluation of a compressed air energy storage system integrated with an organic Rankine cycle

Hui Meng<sup>1</sup>, Meihong Wang<sup>1</sup>, Mathew Aneke<sup>1</sup>, Xiaobo Luo<sup>1</sup>, Olumide Olumayegun<sup>1</sup>, Xiaoyan Liu<sup>2</sup>

1. Department of Chemical and Biological Engineering, Faculty of Engineering, The University of Sheffield, Sheffield, S1 3JD, UK.
2. State Key Laboratory of Chemical Engineering, Department of Chemical Engineering, Tsinghua University, Beijing, 100084, China.

## Abstract

Energy storage becomes increasingly important in balancing electricity supply and demand due to the rise of intermittent power generation from renewable sources. The compressed air energy storage (CAES) system as one of the large scale (>100MW) energy storage technologies has been deployed in Germany and the USA. However, the efficiency of current commercial CAES plants still needs to be improved. In this study, an integrated system consisting of a CAES system and an organic Rankine cycle (ORC) was proposed to recover the waste heat from intercoolers and aftercooler in the charging process and exhaust stream of the recuperator in discharging process of the CAES system. Steady state process models of the CAES system and ORC were developed in Aspen Plus<sup>®</sup>. These models were validated using data from the literature and the results appear in a good agreement. Process analysis was carried out using the validated models regarding the impact of different organic working fluids (R123, R134a, R152a, R245fa, R600a) of ORC and expander inlet pressures of the ORC on system performance. It was found that integrating ORC with the CAES system as well as selecting appropriate working fluid was a reasonable approach for improving performance of the CAES system. The round-trip efficiency was improved by 3.32 - 3.95% using five working fluids, compared to that of the CAES system without ORC. Economic evaluation on levelized cost of electricity (LCOE) was performed using Aspen Process Economic Analyser<sup>®</sup> (APEA). Different working fluids in ORC and different power sources (e.g. wind and solar) associated with the integrated system were considered to estimate the LCOEs. It was found that the LCOEs for the integrated system were competitive with fossil-fuel fired power and even lower

than offshore wind power and solar power. The proposed research presented in this paper hopes to shed light on how to improve efficiency and reduce cost when implementing CAES.

**Keywords:**

Energy Storage; Compressed Air Energy Storage (CAES); Organic Rankine Cycle (ORC); Process Simulation; Economic Evaluation

**Nomenclature**

$W_t$	Output power of Turbine (kWh)
$W_e$	Electrical energy taken from grid for driving the compressors (kWh)
$E_f$	Thermal energy of fuel consumed (kWh)
$\eta_{sys}$	System electric efficiency
$\eta_{eff\_1}$	Round-trip efficiency of the CAES system
$\eta_{eff\_2}$	Round-trip efficiency of the CAES system with system electric efficiency
$W_{ORC\_1}$	Power output of ORC during charging period of the CAES system (kWh)
$W_{ORC\_2}$	Power output of ORC during discharging period (kWh)
$W_{p\_1}$	Power consumption of ORC pump during charging period (kWh)
$W_{p\_2}$	Power consumption of ORC pump during discharging period (kWh)
$\eta_{CAES+ORC}$	Round-trip efficiency of the integrated system based on reducing the electricity taken from grid
$\eta'_{CAES+ORC}$	Round-trip efficiency of the integrated system based on the round-trip efficiency of the CAES system
$P_{EIP}$	ORC expander inlet pressure (bar)
$E_{output}$	Net power output annually of the integrated system
CAES	Compressed air energy storage
ORC	Organic Rankine cycle
LCOE	Levelized cost of electricity

PHS	Pumped hydroelectric storage
LPC	Low pressure compressor
HPC	High pressure compressor
LPT	Low pressure turbine
HPT	High pressure turbine
V	Valve
TAC	Total annual cost
ACAPEX	Annualised capital expenditure
FOPEX	Fixed operation expenditure
VOPEX	Variable operational expenditure
CRF	Capital recovery factor
CAPEX	Capital expenditure
$n$	CAES plant life time
$i$	Discount rate

## 1. Introduction

### 1.1 Background

With the increase in global electrical energy demand, the annual amount of electricity generation reached more than 22,000 TWh in 2012. Power generation from fossil fuels contributes to approximately 70% worldwide electricity energy supply [1,2]. As a result, massive CO<sub>2</sub> emission released to the atmosphere has led to the problem of greenhouse effect [3]. To reduce the CO<sub>2</sub> emission and also the dependence on fossil fuels, renewable energies have been considered as alternative sources such as solar, wind and tide power [1,4]. However, the majority of renewable energies have a common problem of intermittence, which brings a great challenge to ensure the stability and reliability of the electricity grid [2,4,5]. Electrical energy storage as one of the most promising methods to address the problem has become increasingly important in balancing supply and demand of electricity [4,6].

Electrical energy storage refers to a process of transforming energy from electrical energy into a form which can be stored and converted back into electrical energy when needed [2,7]. Many energy storage technologies have been developed such as pumped hydroelectric storage (PHS), compressed air energy storage (CAES), batteries, fuel cells, superconducting magnetic energy systems, flywheel, capacitors and supercapacitors [2,4–9]. Presently, only PHS and CAES technologies can be applied in large (e.g. grid) scale (> 100MW) application. The PHS technology is mature and has been implemented widely [2,4,10,11]. Nevertheless, geographical constrains for PHS plants requiring two large reservoirs at different elevations limit its commercial deployment [7,9,12,13]. Thus, CAES technology could become an attractive alternative for large or grid scale energy storage.

### 1.2 Literature review

CAES technology began to be attractive by the mid-1970s [14]. The CAES system can be implemented at different scales of capacities. The advantages of large-scale CAES systems integrated with the grid network include peak shaving, load shifting, frequency and voltage control [10,11]. CAES plants also can be integrated with intermittent renewable energy, such as

wind and solar power, to smooth the output power [10]. In addition, Bouman presented that the environmental impacts of CAES plants are lower than that of natural gas power plants [15]. However, the major constraints of the CAES system are the geographical requirement of the proper cavern and combustion of fossil fuel in the discharging process [7,10].

The Huntorf CAES plant in Germany, as the first commercial plant in the world, has been operated since 1978 [11,16]. The Huntorf CAES plant has 290MW output power for ~2-hour discharging duration. Compressed air is stored in two caverns ( with total volume around 310,000m<sup>3</sup> ) with about 43-70bar operating pressure and a depth of around 600m [7,17,18]. It is reported that the Huntorf CAES plant has operated with remarkable performance with ~90% availability and ~99% starting reliability [7,10]. The round-trip efficiency of the plant is around 42% [10,19]. The second CAES plant has been operated since 1991 in McIntosh, Alabama, USA. The McIntosh CAES plant can generate 110MW output power for around 26-hour discharging duration. The storage capacity of the cavern is over 500,000m<sup>3</sup> with operating pressure of 45-74bar and a depth of around 450m [7,10,18]. Comparing the two commercial CAES plants, the major improvement of the McIntosh CAES plant is the use of a recuperator to recover waste heat from turbine exhaust to preheat compressed air, which can increase round-trip efficiency from 42% to 54% and also reduce fuel consumption by 22-25% [10]. In 2016, a 10MW advanced CAES system was implemented by the Energy Storage R&D Centre, Chinese Academy of Science in Bijie, Guizhou Province, China [20]. The aim of this project is scientific research and demonstration. The main components of the demonstration plant include wide-load compressor, high-load turbine and heat exchangers [20].

The round-trip efficiencies of current commercial plants are still insufficient and need to be improved. As for the further development of CAES technology, adiabatic CAES (A-CAES) technology was initiated in 2003 [14]. A-CAES aims for around 70% round-trip efficiency of A-CAES [10,14]. The strength of A-CAES technology can be high round-trip efficiency and emission-free (no fuels used in the discharging process); thermal energy storage (TES) is implemented for storing the heat from the charging process and reusing it during the discharging process in A-CAES system [14,21,22]. However, the technical cases and commercialised A-CAES plants about specific operating conditions have not been deployed so far; because the major challenges are the complex system engineering and adiabatic compressor combined with high-temperature TES, special materials could be required to overcome the thermal and mechanical stress [14,21,22].

Currently, some CAES systems are under research and development, such as Norton 2700MW (3×900MW) CAES project [7,14], Iowa 270MW CAES project [23], Texas 317MW CAES project [14], UK Larne 330MW (2×165MW) CAES project [14,24]. Some studies investigated process performance, components and the integrated system of the CAES system using different simulation tools, such as CFD (computational fluid dynamics) [25–28], Aspen Plus [29,30], Matlab/Simulink [31–35]. In the literatures, the approaches used to improve round-trip efficiencies of CAES systems emphasise the waste heat recovery from compressors in charging process and turbine in discharging process of the CAES system. A detailed process description of the CAES system is given in Section 2.1.

Organic Rankine cycle (ORC) has beneficial impacts on the energy efficiency through waste heat recovery [34,36]. Integrating an ORC with a system to convert waste heat into electrical energy could enable this system to achieve better performance [34,37–39]. The major advantages of the ORC include low mechanical stress, high efficiency of turbine, low operation cost and long plant life [40]. Also, Liu et al. investigated that the payback time of some pollutant gases CO<sub>2</sub>, CH<sub>4</sub> and NO<sub>x</sub> in the ORC for waste heat recovery life cycle can be shorter, compared with the grid emission of other five types of power generation modes [41]. ORC technology has been investigated since the 1880s, it could be implemented to recover low grade energy from different power systems, such as industrial waste heat solar energy, biomass, geothermal energy, fuel cells and ocean thermal energy [34,36,42–45]. ORC application with 0.2-2MW output power has been validated in several industrial plants installed in the USA, Germany, Italy, Netherlands, Austria and Sweden [36,42]. Several commercial ORC projects have been established in the world with the power output range from kW to 10MW using different working fluids and operating temperatures [36,46]. The selection of appropriate working fluids in ORC is crucial because it can have significant effects on the system performance [42]. A number of studies has reported that the selection of working fluids of ORC depends on the heat recovery applications and multiple criteria, such as low-toxicity, low-flammability, high flash point, pressure, curve of saturation and low cost etc. [36,40,42,44,47]. Pezzuolo et al. [40,48] analysed different working fluids of ORC recovering heat from different heat sources based on simulation. The analysis results on different working fluids for an ORC integrated with solar energy were summarised in [40]. The detailed description of ORC is given in Section 2.2.

### 1.3 Motivation

With regards to waste heat from charging and discharging processes in the CAES system, the temperatures of inter-coolers, after-cooler and exhaust from recuperator (from 95 °C to 130°C) are high enough to be recovered for power generation using an ORC. CAES system integrated with ORC for waste heat recovery will also improve the round-trip efficiency of the CAES system. Therefore, the integration of the ORC to recover waste heat from charging and discharging processes of the CAES system is investigated and analysed through process simulation for improving system performance in this study.

### 1.4 Aims and novel contributions

This study aims to improve the technical performance and perform economic evaluation of the CAES system by proposing the integration of ORC with the CAES system to recover waste heat from inter-coolers and after-cooler in charging process and exhaust of recuperator in discharging process of the CAES system. A steady state model developed in Aspen Plus® and the process models of the CAES system and the ORC has been validated. The main contributions of this study include:

- A new scheme for waste heat recovery was proposed for the CAES system
- The process performance was analysed through process simulation using the validated models
- Economic evaluation of the integrated system using Aspen Process Economic Analyser® (APEA)

This study investigated the technical performance of the integrated system, as well as the economic evaluation of the integrated system with different working fluids of ORC and different power sources associated with the integrated system. It was found that integrating ORC with the CAES system as well as selecting appropriate working fluid is reasonable approach for improving performance of the CAES system. The round-trip efficiency was improved by 3.32% - 3.95% using five working fluids, compared to that of the CAES system without ORC. It is also found that LCOE of the CAES system integrated with the ORC is cheaper than some renewable energy (e.g. offshore wind power and solar power) and the LCOE of the CAES system integrated with the ORC

associated with renewable energy is cheaper than that of the CAES system without the ORC. The models of the CAES system were validated with both real plant data and literature data to ensure the accuracy of the simulations. The model of the ORC was also validated with real plant data.

## 2. Process description

### 2.1 Process description of CAES

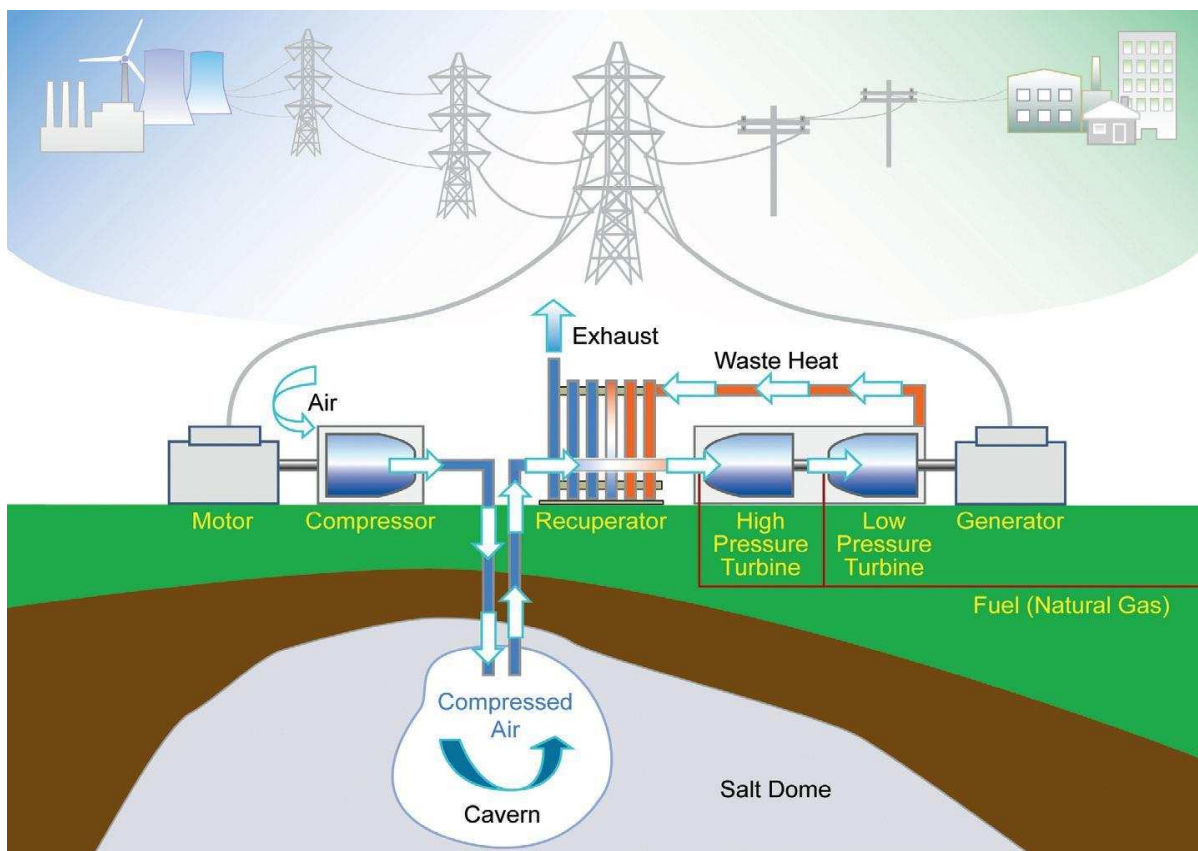


Fig. 1. A schematic diagram of a CAES process [49]

A CAES process (Fig. 1) consists of three main subsystems: air charging, compressed air storage and compressed air discharging subsystems. In the charging subsystem, excess electricity at off-peak time is utilised to compress air. The compressed air is injected into underground storage at high pressure. In the discharging subsystem, the stored compressed air in the cavern is extracted for generating electricity. The compressed air extracted is first preheated in the recuperator with

recovering waste heat from the exhaust of the low-pressure turbine before the waste heat is released to the atmosphere. The preheated air then passes into the combustion chambers where it is mixed with fuel (e.g. natural gas) to be combusted. The high temperature combustion product is expanded in the turbines to produce electricity [10,11,50].

## 2.2 Process description of ORC

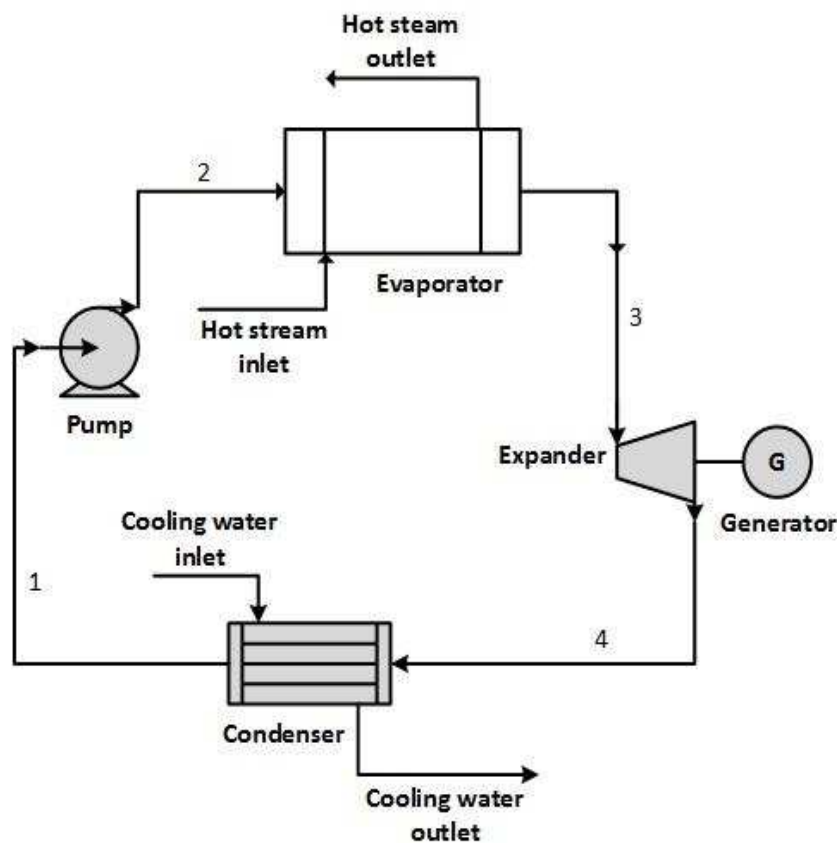


Fig. 2. A schematic diagram of ORC process [51]

ORC works on the principle (Fig. 2) of using an organic fluid with boiling point less than that of water as the working fluid. Recovering low-grade waste heat ( $T < 370^{\circ}\text{C}$ ) from other systems by integrating ORC can improve the performance of the entire system [34,37–39]. The main components of an ORC are evaporator, expander, condenser and pump. The working fluid leaving the condenser is compressed by a pump and fed back to the evaporator for recovering waste heat. The working fluid will be evaporated. The evaporated vapour passes into the expander to generate electricity by rotating the shaft, which is connecting to the generator. Finally, the

exhaust from expander will be condensed from vapour to liquid in the condenser using cooling water [43].

### 2.3 Description of the integrated system for waste heat recovery

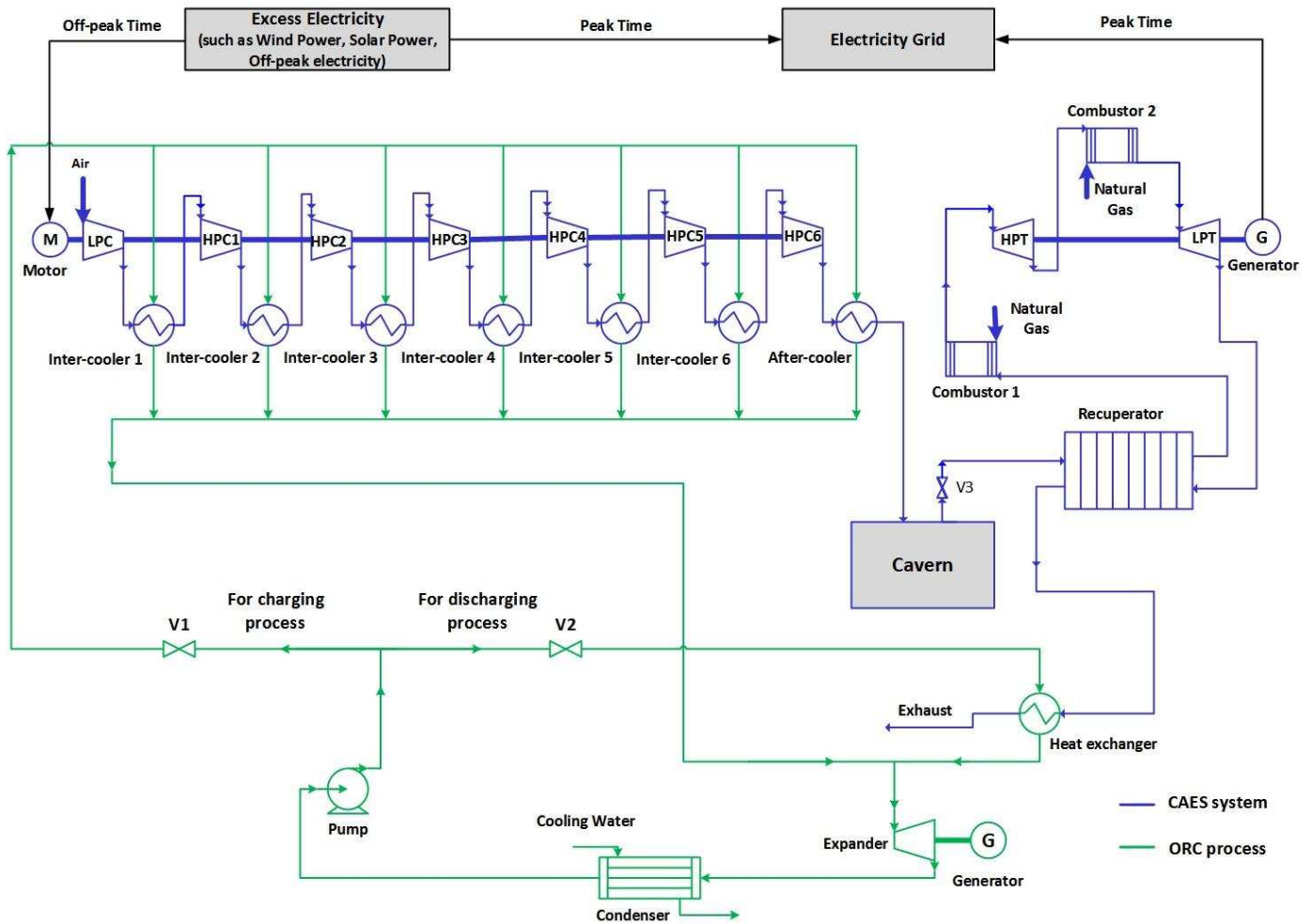


Fig. 3. Schematic diagram of CAES system integrated with ORC

The schematic diagram of the proposed CAES system integrated with the ORC is shown in Fig. 3. The organic working fluid of the ORC has two flow path options for heat recovery in the integrated system, because charging and discharging operations do not occur simultaneously. During the charging operation of the CAES system in off-peak period, the organic working fluid in the ORC will flow through V1 to recover waste heat from the intercoolers and aftercooler of the compressors to generate electricity for reducing the electrical energy taken from grid for driving

the compressors. During the discharging operation of the CAES system in peak period, the organic working fluid will flow through V2 to recover waste heat from the exhaust gas leaving the recuperator to generate more electricity for the improvement of system performance. Therefore, an ORC integrated with the CAES system can recover waste heat during both charging and discharging operations. This can improve the efficiency as well as reduce the operating cost of the system. Similar as Columbia Hills CAES system from the Pacific Northwest National Laboratory (PNNL) technical report, 3 hours per day of the charging operation and 6 hours per day of the discharging operation were specified in this study [52].

It was noticed that an ORC would have different operating points during charging and discharging operations because of the different flowrates, operating pressures and temperatures. This will affect the design of the ORC components, especially the ORC expander. Hence, there will be two ORC expanders in real applications, although the process diagram (Fig. 3) shows only one ORC expander. Two expanders will be engaged during the charging operation period. However, one of expanders will be withdrawn during the discharging operation because the recovered waste heat during discharging period is less than that during the charging period. This situation was taken into consideration for the economic evaluation of the integrated system in Section 5.2.

### **3. Process model development**

The methodology used in this study is a typical process simulation approach followed by an economic evaluation. Process models of the CAES system and the ORC were developed and simulated in Aspen Plus® V8.4 with input parameters based on industrial operation consideration.

#### **3.1 Model development of the CAES system**

The CAES model can be divided into two sections: air charging and compressed air discharging sections. The model consists of the main components such as air compressor, intercooler, aftercooler, tank, recuperator, combustor and turbine. The compressors and turbines were simulated based on isentropic efficiency using *Compr* block in Aspen Plus®. Isentropic efficiencies and mechanical efficiencies of compressors and turbines were specified to improve the accuracy

of the prediction [53,54]. The intercoolers and aftercooler were simulated with *Heater* blocks, which was selected by heat transfer between process stream and cooling utility. The outlet temperature and pressure were required for implementing this block in the CAES model. The combustor was simulated with *RGibbs* reactor block. The flowrate of air should be ensured with complete (equilibrium) combustion of the natural gas. The *RGibbs* block calculates the equilibriums by the Gibbs free energy minimisation thereby avoiding the complicated calculations of reaction stoichiometry and kinetics. This will simplify the required input parameters for the block. Phase equilibrium and chemical equilibrium was selected as the calculation option for the combustors and the required inputs were temperature and heat duty of the combustor. The storage tank was simulated with *Mixer\_Tank* block and the required input was outlet pressure of the tank. The recuperator was simulated with a *HeatX* block, because two process streams for heat transfer were specified. The flow direction in the recuperator was chosen to be counter-current flow. The selected input parameters and options for exchanger specifications were design option, exchanger duty and minimum temperature approach. PENG-ROB (Standard Peng-Robinson cubic equation of state) method was implemented for the property calculation for the CAES model [29]. Different components of the CAES system and corresponding blocks in Aspen Plus® has been summarised Table 1.

Table 1. Summary of components of the CAES system and corresponding blocks in Aspen Plus®

Components	Blocks in Aspen Plus®
Compressors / Turbines	<i>Compr</i>
Intercoolers / Aftercooler	<i>Heater</i>
Combustors	<i>RGibbs</i>
Storage Tank	<i>Mixer_Tank</i>
Recuperator	<i>HeatX</i>

### 3.2 Model development of the ORC

The modelled components of the ORC include pump, evaporator, expander and condenser. The pump was simulated with *Pump* block in Aspen Plus® and discharge pressure was supplied as input parameter. The expander was simulated as isentropic turbines using *Compr* block. The

requirement for this block is same as the compressor or turbine in the CAES model. The evaporator and condenser were simulated with *HeatX* block which is same as the requirement of the recuperator in the CAES model. The flow direction and input parameters specification type were chosen to be countercurrent and design respectively. Minimum temperature approach was specified as input parameter for both the evaporator and the condenser. Different components of the ORC and corresponding blocks in Aspen Plus® has been summarised Table 2.

Table 2. Summary of components of the ORC and corresponding blocks in Aspen Plus®

Components	Blocks in Aspen Plus®
Pump	<i>Pump</i>
Expander	<i>Compr</i>
Evaporator / Condenser	<i>HeatX</i>

### 3.3 Performance criteria

#### 3.3.1 Round-trip efficiency of CAES system

The system performance criteria of the CAES system is different from other power plants because two different types of input energy are consumed during the charging and discharging periods. One is the electrical energy used for driving the compressors during the charging period and another is thermal energy of fuel combusted to heat compressed air before expansion in the turbines during the discharging period. There are two different Equations (1) & (2) to calculate the round-trip efficiency of the CAES system  $\eta_{eff}$ . A broad overview of these two methods has been described in [14,50,29,55].

$$\eta_{eff\_1} = \frac{W_t}{W_e + E_f} \quad (1)$$

$$\eta_{eff\_2} = \frac{W_t}{W_e + \eta_{sys} \cdot E_f} \quad (2)$$

Where,

$W_t$  = Output power of Turbine (kWh);

$W_e$  = Electrical energy taken from grid for driving the compressors (kWh);

$E_f$  = Thermal energy of fuel consumed (kWh);

$\eta_{sys}$  = System electric efficiency

According to equation (1), both input energy are regarded as charging energy, this method is commonly adopted by many studies [14,50,29]. As for Equation (2), the value of thermal energy contribution of fuel consumed is reduced by a reference system electric efficiency. The value  $\eta_{sys}$  depends on the common gas firing conversion systems. In general, the system electric efficiency of these systems could be between around 30% and 50% [50,56]. However, Equation (1) is using the measurable inputs energy and it is convictive for comparison in the efficiencies of different CAES systems [14]. Thus, Equation (1) will be used for the following calculations of round-trip efficiency of the CAES system.

### 3.3.2 Round-trip efficiency of the integrated system

Based on equation (1), the general round-trip efficiency of the integrated system of the CAES system with the ORC based on the round-trip efficiency of the CAES system could be described as:

$$\eta'_{CAES+ORC} = \frac{W_t + W_{ORC\_1} + W_{ORC\_2}}{E_f + W_e + W_{p\_1} + W_{p\_2}} \quad (3)$$

Where,

$W_{ORC\_1}$  = Power output of ORC during charging period of the CAES system (kWh)

$W_{ORC\_2}$  = Power output of ORC during discharging period (kWh)

$W_{p\_1}$  = Power consumption of ORC pump during charging period (kWh)

$W_{p\_2}$  = Power consumption of ORC pump during discharging period (kWh)



The plant data used for the Huntorf CAES model validation was obtained from Crotigino et al. [16], Liu et al. [29] and Hoffein [57]. The flowsheet of Huntorf CAES system is shown in Fig. 4. Table 3 gives the input process conditions and parameters of the Huntorf CAES plant model.

Table 3. Input process conditions and parameters of Huntorf CAES plant model

Stream Numbers	Process Conditions			
	Process Point Description	Pressure (bar)	Temperature (°C)	Flowrate (kg/s)
1	Ambient conditions	1.013	10	108
2	Outlet 1 <sup>st</sup> compressor	6		108
3	Outlet 2 <sup>nd</sup> compressor	46		108
4	Aftercooler outlet / Cavern inlet		50	108
5	Throttle outlet	42		417
6	Inlet 1 <sup>st</sup> turbine	42	550	417
7	Inlet 2 <sup>nd</sup> turbine	11	825	417
8	Outlet 2 <sup>nd</sup> turbine	1.13		417
	Compressor isentropic efficiency		75%*	
	Turbine isentropic efficiency		85%*	

\* The efficiencies were calculated regressively from data set

In Table 4, the simulation results were compared with the Huntorf CAES plant data [57]. The results show that relative errors are 1.72% and 3.05%. However, only two variables, consumption power of compressors and output power of turbines were compared with simulation results, due to lack of detailed data in the literatures [16,50,29,57,58].

Table 4. Simulation results compared with the plant data for Huntorf CAES plant

Variables	Plant Data [57]	Simulation Results	Relative Errors (%)
Consumption Power of Compressors (MW)	60	61.03	1.72
Output Power of Turbines (MW)	290	298.84	3.05

#### 4.2 Model comparison of Columbia Hills CAES project

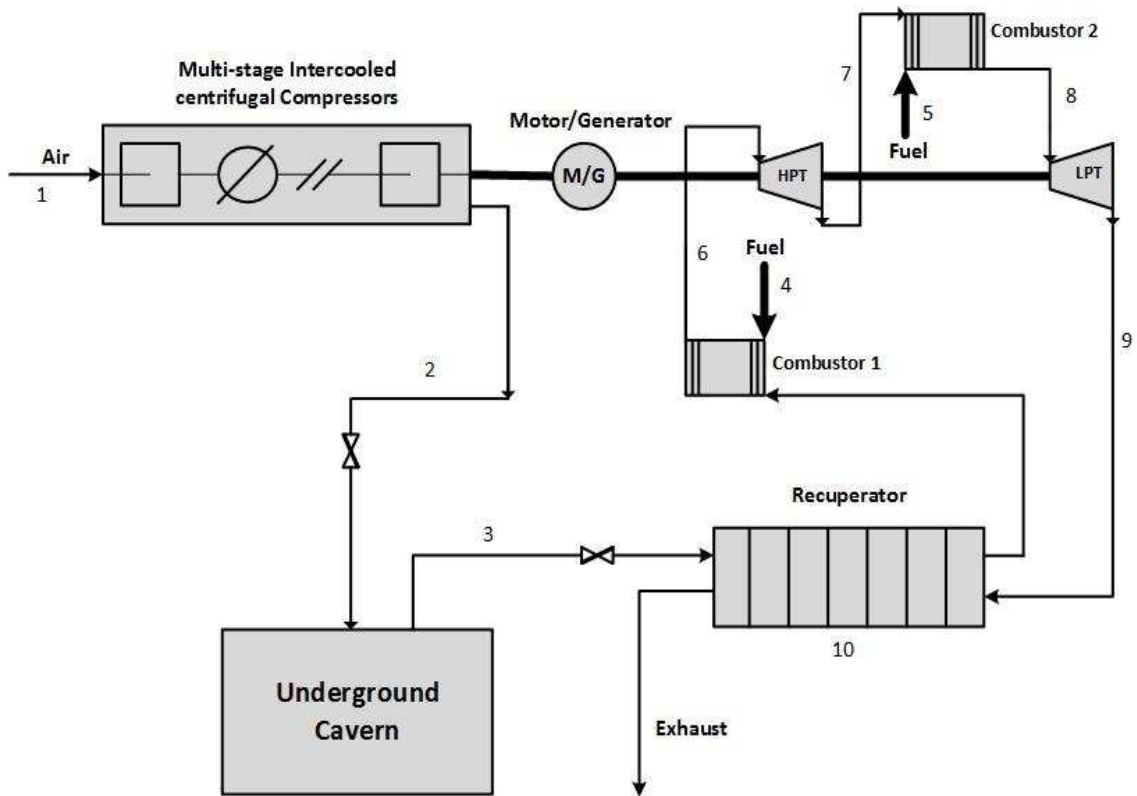


Fig. 5. Columbia Hills CAES system process flow diagram [52]

The flowsheet and simulation data for the Columbia Hills CAES plant were obtained from a technical report by PNNL [52]. Fig. 5 shows the process configuration of the Columbia Hills CAES system. The main difference between the Columbia Hills CAES system and the Huntorf CAES system is a recuperator which can recover the heat from exhaust of turbine for preheating compressed air. The Charging process at the Columbia Hills CAES system is implemented with a

multi-stage centrifugal compressor with six intercooled stages [52]. Using intercooled centrifugal compression stages can reduce the gross energy demand of the machine and therefore improves efficiency. However, this increases the capital cost when compared to the Huntorf CAES plant. The simulation results will be compared with the literature data [52]. Table 5 gives the input process conditions and parameters of the Columbia Hills CAES project.

Table 5. Input process conditions of Columbia Hills CAES system

Stream Numbers	Process Conditions			
	Process parameters	Pressure (bar)	Temperature (°C)	Flowrate (kg/s)
1	Ambient conditions	1.03	15	353
2	Aftercooler exit / Cavern inlet	115.65		353
3	Throttle outlet	35.78	40.56	189
4	Inlet natural gas of 1 <sup>st</sup> combustor	44.82	32.22	0.527
5	Inlet natural gas of 2 <sup>nd</sup> combustor	24.13	32.22	4.111
6	Inlet 1 <sup>st</sup> turbine/Outlet of 1 <sup>st</sup> combustor	34.40		
7	Outlet 1 <sup>st</sup> turbine	18.27		
8	Inlet 2 <sup>nd</sup> turbine/Outlet 2 <sup>nd</sup> combustor	17.93		
9	Outlet 2 <sup>nd</sup> turbine	1.03		
10	Heat duty of recuperator (MW)	105.51		
	Air charging time (Hours)		3	
	Compressed air discharging time (Hours)		6	
	Pressure ratio of compressor		1.96177*	
	Compressor isentropic efficiency		75%*	
	Turbine isentropic efficiency		93%*	

\* The pressure ratio and efficiencies were calculated regressively from data set

In Table 6, the model simulation results are compared with the literature data. The results for the Columbia Hills CAES system model simulation showed that for all runs the relative errors is less than 0.7% except the error prediction of exhaust temperature of the recuperator which is 4.64%.

Table 6. Simulation results compared with literature data for Columbia Hills CAES system

Parameters / Variables	Literature Data [52]	Simulation Results	Relative Errors (%)
Temperature of Aftercooler exit / Cavern inlet (°C)	40.56	40.56	0.00
Cold stream outlet temperature of recuperator (°C)	562.78	560.12	0.47
Temperature of inlet 1 <sup>st</sup> turbine / outlet of 1 <sup>st</sup> combustor (°C)	676.67	673.89	0.41
Temperature of outlet 1 <sup>st</sup> turbine (°C)	546.11	544.02	0.38
Temperature of inlet 2 <sup>nd</sup> turbine / outlet 2 <sup>nd</sup> combustor (°C)	1331.67	1330.65	0.08
Temperature of outlet 2 <sup>nd</sup> turbine (°C)	601.72	605.15	0.57
Exhaust temperature of recuperator (°C)	115.56	120.92	4.64
Consumption Power of Compressors (MW)	228.67	230.22	0.68
Output Power of Turbines (MW)	205.39	205.76	0.18

#### 4.3 Model validation of the ORC

The flowsheet (refer to Fig. 2) and plant data for validation of the ORC model were obtained from the Chena Geothermal Power Plant [51]. The organic working fluid of the ORC is R134a (1,1,1,2-tetrafluoroethane). It is a common refrigerant implemented in a wide range of refrigeration and air conditioning applications, including medium and high temperature refrigeration and industrial applications [59]. Table 7 gives the input process conditions of the ORC.

Table 7. Input process conditions and parameters of the ORC

Parameters / Variables	Plant Data
Hot stream inlet mass flowrate (kg/s)	33.39
Hot stream inlet temperature (°C)	73.33
R134a mass flowrate (kg/s)	12.17
Cooling water inlet mass flowrate (kg/s)	101.68
Cooling water inlet temperature (°C)	4.44
Turbine inlet / outlet pressure (bar)	16.00 / 4.00
Pump efficiency	90%
Expander efficiency	80%

The simulation results were compared with the plant data for model validation as shown in Table 8. All the relative errors were less than 6.02% and the simulation results matched the real plant data.

Table 8. Simulation results compared with ORC data from the Chena Geothermal Power Plant

Parameters / Variables	Literature data [51]	Simulation results	Relative Errors (%)
Hot stream outlet temperature (°C)	54.44	55.27	1.52
Cooling water outlet temperature (°C)	10.00	9.82	1.80
Output power of Expander (kW)	250.00	252.56	1.02
Evaporator heat transfer rate (kW)	2580.00	2735.33	6.02
Condenser heat transfer rate (kW)	2360.00	2482.32	5.18

## 5. Results and discussion

### 5.1 Process analysis and technical performance evaluation of the integrated system

This section will discuss and analyse the effects of different ORC working fluids and expander inlet pressure (EIP) on the system performance. Some assumptions for the analysis of the proposed integrated system are:

- The fuel used in the CAES discharging process was assumed to be 100 vol% methane.
- The pressure drops of all components were ignored.
- The temperature of condenser cooling water was assumed to be 10°C.
- The working fluid at outlet of the condenser was saturated liquid and the temperature was around 20°C.
- The exhaust gas at outlet of evaporator during discharging period is 100% vapour fraction and the temperature was assumed to be 45°C.
- The isentropic efficiencies of ORC expander and pump were assumed to be 93% and 90% respectively [51,60].

- The minimum temperature approaches of ORC evaporators (intercoolers and aftercooler) and condensers were assumed to be 3°C [61–64].

### 5.1.1 Effects of the ORC organic working fluid

Selection of the working fluid is important for improving performance of the ORC [34,40,42,43]. Different working fluids would have different impacts on the power output and the round-trip efficiency. Therefore, it is essential to investigate effects of different organic working fluids on the ORC power output and the round-trip efficiency of the integrated system.

For this case study, the performance of following refrigerants as working fluids in the ORC will be compared: R123 (2, 2-dichloro-1, 1, 1-trifluoroethane), R134a (1, 1, 1, 2-tetrafluoroethane), R152a (1, 1-difluoroethane), R245fa (1, 1, 1, 3, 3-pentafluoropropane) and R600a (isobutene). The thermo-physical properties of these refrigerants listed in Table 9 are calculated by REFROP V9.1. The input conditions for the CAES system were shown in Table 5.

Table 9. Thermo-physical properties of different refrigerants

Refrigerants	Molecular Mass (kg/kmol)	Boiling Point (°C)	Critical Pressure (bar)	Critical Temperature (°C)
R123	152.93	27.82	36.62	183.68
R134a	102.03	-26.07	40.60	101.06
R152a	66.05	-24.02	45.17	113.26
R245fa	134.05	15.14	36.51	154.01
R600a	58.12	-11.75	36.29	134.66

Table 10. Process simulation results of the integrated systems using different working fluids

	R600a		R245fa		R152a		R134a		R123	
Variables	Charging	Discharging								

<b>EIP* (bar)</b>	17.40	24.60	10.70	18.40	30.90	45.10	34.70	40.00	6.71	11.50
<b>EIT* (°C)</b>	92.90	111.58	92.93	117.79	93.14	113.17	93.07	100.31	93.19	117.85
<b>Mass flow rate (kg/s)</b>	515.26	36.53	883.83	61.49	689.24	58.90	1092.51	86.99	1006.80	69.76
<b>W<sub>ORC_1</sub> or W<sub>ORC_2</sub> (MW)</b>	33.25	2.78	33.24	2.89	33.97	2.72	32.49	2.42	34.36	3.01

\* EIP and EIT are ORC expander inlet pressure and temperature respectively.

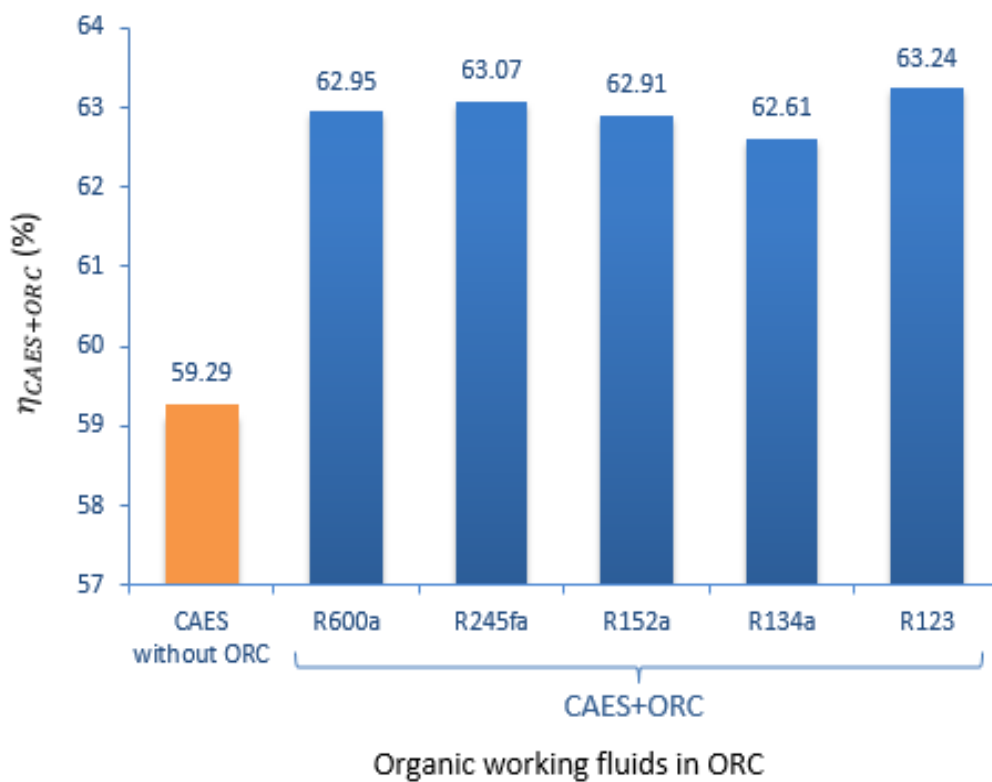


Fig. 6. Round-trip efficiency of the CAES system and the integrated system using different working fluids

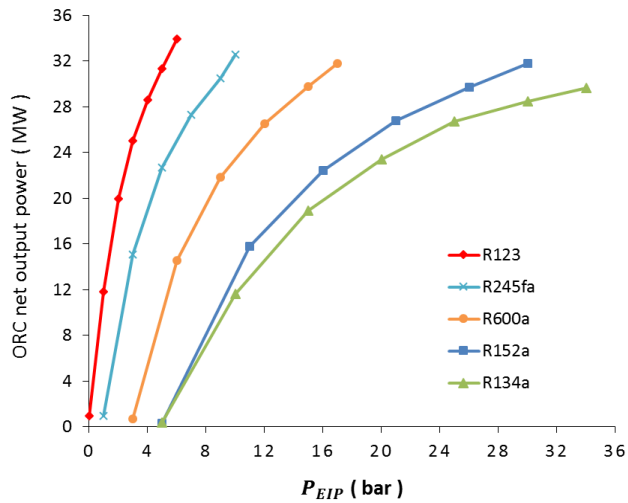
Table 10 presents the simulation results of the integrated systems using different organic working fluids in the ORC. In conventional steam Rankine cycle, water as the common working fluid is used to recover waste heat. However, the temperature of waste heat could be not high enough to superheat water and if outlet stream of the ORC expander contains more than 15% saturated

liquid, this could damage ORC expander blades and reduce efficiency of the expander [65]. The organic working fluid does not have this problem because the organic working fluid does not need to be superheated and the outlet stream of the ORC expander can be always saturated vapour [36,42,65]. From the results in Table 10, R123 gives the highest ORC power output in both charging and discharging operations of the CAES system because the high critical temperature of the working fluid could improve the system performance [34,37]. A high critical temperature also could result in low vapour densities, this can lead to the high cost. The results showed that there are significant differences in ORC EIP, the effect of the EIP on the system performance will be discussed in section 5.1.2.

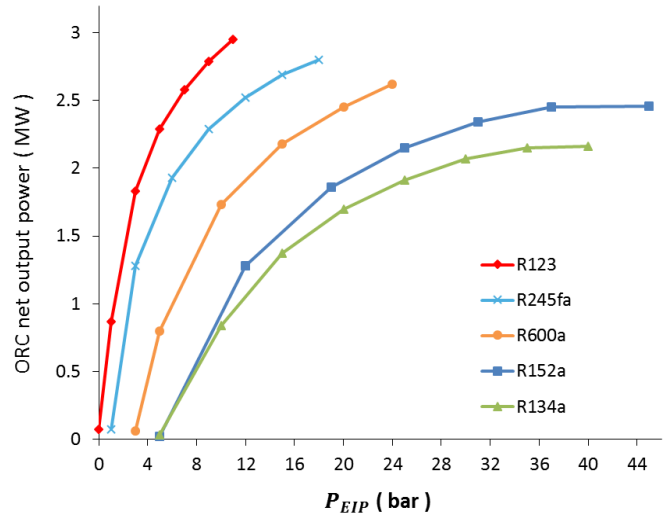
Fig. 6 presents round-trip efficiencies of the standalone CAES system and the integrated system using different ORC working fluids. The round-trip efficiency of the CAES system without the ORC was 59.29% calculated by Equation (1). Round-trip efficiencies of the integrated system using different working fluids were 62.95% (R600a), 63.07% (R245a), 62.91% (R152a), 62.61% (R134a) and 63.24% (R123) respectively, which were calculated by Equation (4). It is evident from Fig. 6 that round-trip efficiencies of the integrated system using different working fluids increased by 3.32 - 3.95%, when integrating with the ORC. Therefore, integrating the ORC with the CAES system as well as selecting appropriate working fluid is reasonable approach for improving performance of the CAES system.

### 5.1.2 Effects of expander inlet pressure (EIP) of the ORC

The EIP of the ORC should be considered since the pressure ratio of the expander will significantly affect the output power of the ORC. Therefore, it is essential to investigate the relationships of EIP of different working fluids and the ORC power output during charging and discharging periods. The input conditions were same as Section 5.1.1.

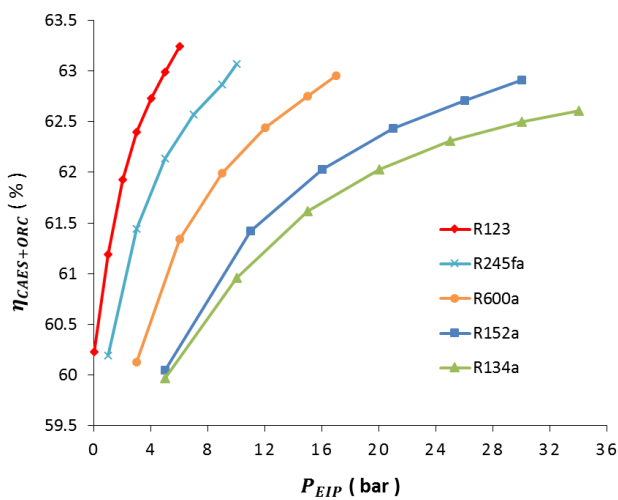


(a)

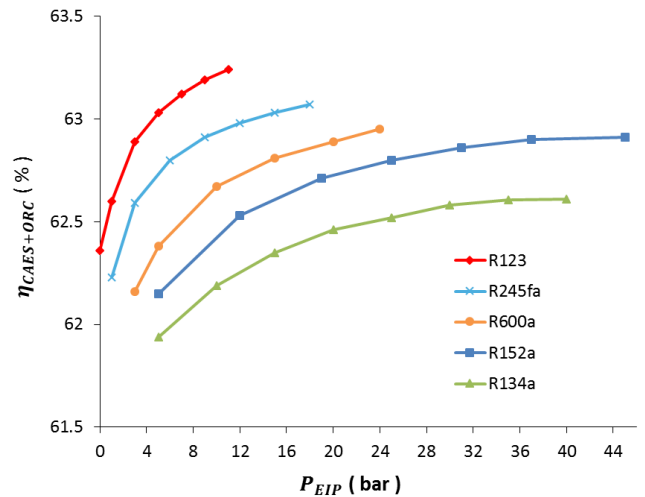


(b)

Fig. 7. Effect of EIP on ORC net power output during (a) charging and (b) discharging processes



(a)



(b)

Fig. 8 Effect of EIP on the round-trip efficiency of the integrated system during (a) charging and (b) discharging processes

Fig. 7 indicates the variation of the ORC net power output with the EIP during (a) charging and (b) discharging processes. An increase in the EIP leads to the increase of ORC power output using these five different working fluids. This is because with the fixed expander outlet pressure, a higher EIP will mean a higher pressure ratio of the expander leading to a larger enthalpy drop through the expander. Fig. 8 presents the variation of the round-trip efficiency of the integrated

system with the EIP of the ORC during charging and discharging processes. A higher EIP will lead to an increase in the ORC net power output. The Round-trip efficiencies of both Fig. 8 (a) and (b) were calculated by Equation (4). The Round-trip efficiencies in Fig. 8 (a) were calculated by varying the EIP of the expander during charging process while the EIP of the expander during discharging process was fixed at the best operating point. Conversely, the round-trip efficiencies in Fig. 8 (b) were calculated by varying the EIP of the expander during discharging process while the EIP of the expander during charging process was fixed at the best operating point.

From the results of Fig. 7, the EIP of using R134a and R152a as ORC working fluids servicing to discharging operation of the CAES system could be not appropriate because the EIP of using them implemented to achieve the best net power output has already reached their critical pressures (refer to Table 9). R123 as the ORC working fluid can generate the highest net power output with the lowest EIP, but the flowrate is not low (refer to Table 10) which could lead to the increase of capital cost. Therefore, selecting an appropriate working fluid considers efficiency and safe operation frequently, economic evaluation should be also an important factor for power plants. Next section will investigate economic evaluation of the integrated system using different ORC working fluids.

## 5.2 Economic Evaluation

### 5.2.1 Economic evaluation methodology

Economic evaluations were implemented in APEA V8.4. APEA has become a professional and industrial standard Engineering tool. It is considered to be more accurate than correlation-based economic evaluation methods [66]. APEA can be used for engineering design and evaluation of different types of projects because it consists of design procedures and price data for many types of project materials and components and considers engineering contingency (5%). A bottom-up method is applied through the APEA. The unit operations were mapped to individual equipment cost model that can be designed manually due to some special components, when the simulation model is imported into APEA.

As for the expenditures, the levelized cost of electricity (LCOE) of the integrated system was calculated through dividing total annual cost (TAC) by the net power output annually ( $E_{output}$ ),

as expressed in Equation (5) [67]. TAC is a sum of annualised capital expenditure (ACAPEX), fixed operation expenditure (FOPEX) and variable operational expenditure (VOPEX), as described in Equation (6) [52,66,67]. CAPEX involves the costs of equipment materials and installation, engineering and management, labour generated during the plant construction. The ACAPEX is the total CAPEX multiplying by capital recovery factor (CRF), as written by Equations (7) and (8) [52,67]. FOPEX involves the costs of long term service agreement, operating and maintenance and other fixed costs which could be generated during the periods of full load or shutdown. VOPEX of this system includes fuel cost and the cost of electricity consumption for the compressors.

$$LCOE = \frac{TAC}{E_{output}} \quad (5)$$

$$TAC = ACAPEX + FOPEX + VOPEX \quad (6)$$

$$ACAPEX = CAPEX \times CRF \quad (7)$$

$$CRF = \frac{i(1+i)^n}{(1+i)^n - 1} \quad (8)$$

CRF is determined by  $n$  (specifying the CAES plant life) and  $i$  (discount rate). Some parameters summarised in Table 11 were used for the LCOE model. Capacity factor is the total time of power output expected in one year. Regarding to the aforementioned equations, a simplified model can be used to calculate the LCOE of the integrated system, described in Equation (9) [52]:

$$LCOE = \{ (CAPEX \times CRF + FOPEX) / (365days \times 24hours \times Capacity\ factor) \} + Fuel\ cost/kWh + Electricity\ consumption\ cost/kWh \quad (9)$$

Table 11. Parameters for LCOE model [52]

Description	Value
CAES plant lifetime (years)	20
Discount rate (%)	4
CRF	0.074
Capacity factor (%)	25
Fuel cost (\$/Thousand Cubic Feet) [68]	3.426
Engineering contingency	5%

### 5.2.2 Economic evaluation of effects of different working fluids of the ORC

For the CAES system integrated with ORC, the investigation of the LCOE with different selection of ORC working fluids is important for comparing their economic advantages. Selection of the working fluid will not only affect the power output and round-trip efficiency, but also affect the cost of the equipment and the plant. Therefore, it is essential to investigate economic impacts of the different ORC working fluids.

The compressors of the charging process will consume electricity to compress air for storing energy. In general, the CAES system uses excess and cheaper electricity to compress air at the off-peak time, due to economical consideration. The electricity price 2.927 cents/kWh at off-peak time in the winter was assumed for this case study [69].

Table 12. Comparison of costs of CAES system integrated with ORC using different working fluids

	<b>R134a</b>	<b>R123</b>	<b>R152a</b>	<b>R245fa</b>	<b>R600a</b>
CAPEX (cents/kWh)	4.880	4.898	4.872	4.910	4.934
FOPEX (cents/kWh)	0.725	0.713	0.722	0.714	0.716
Fuel cost (cents/kWh)	0.0463	0.0462	0.0463	0.0462	0.0463
Electricity consumption cost (cents/kWh)	1.414	1.377	1.397	1.388	1.395
LCOE (cents/kWh)	7.066	7.035	7.037	7.058	7.091

Table 12 illustrates the different costs of CAES system integrated with ORC using different working fluids. FOPEX and Fuel cost are almost the same for the five working fluids because all the components and flow rate of fuel are the same. However, the CAPEX are different because the EIP and EIT of ORC for the different working fluids are different. Hence, the size and capital cost of components are different. Cost of electricity consumption for five different working fluids are different because power outputs for the different working fluids during charging and discharging operations are different. LCOE was lowest with R123 as the working fluid and that of R152a was almost same as R123. However, the round-trip efficiencies of the integrated system for them are

different in Fig. 6. Therefore, round-trip efficiency of a system is not the only factor that should be considered, economic evaluation of the system is also important.

### 5.2.3 Economic evaluation of effects of different power sources

The CAES system integrated with the ORC is not an independent system and it has to be associated with power plants such as coal-fired, wind, nuclear, solar photovoltaic (PV) power plants [7]. Therefore, considering and comparing the effects of the power sources on the price of electricity is essential.

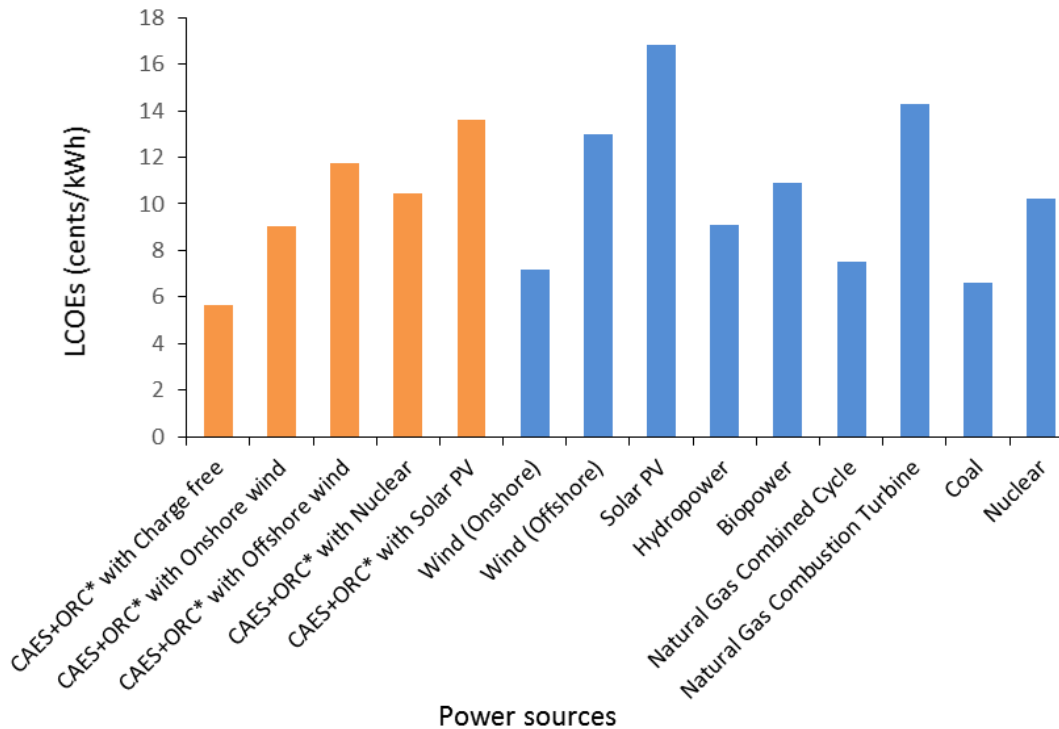
The CAES system without the ORC will be implemented and compared with the integrated system associated with different power sources including charge free, commercial power (off-peak), wind power, nuclear power and solar PV power. Electricity prices of these power sources are different. Therefore, it could be persuasive that LCOEs of the integrated system using different working fluids associated with different power sources was investigated.

Table 13. LCOE of the standalone CAES system and the integrated system associated with different power sources

	Charge free	Commercial power [69]		Wind power [70]		Nuclear power [70]	Solar PV power [70,71]	
		Off-peak in Summer	Off-peak in Winter	Onshore	offshore			
Power price (cents/kWh)	0	7.912	2.927	7.2	13	10.2	16.85	
<b>LCOE (cents/kWh)</b>								
<b>Case 1: CAES without ORC</b>	5.247	9.673	6.885	9.275	12.520	10.953	14.674	
<b>Case 2: CAES with ORC</b>	R134a	5.652	9.474	7.066	9.130	11.932	10.579	13.792
	R123	5.658	9.380	7.035	9.045	11.774	10.456	13.585
	R152a	5.640	9.416	7.037	9.077	11.845	10.508	13.682
	R245fa	5.671	9.422	7.058	9.084	11.834	10.507	13.659
	R600a	5.696	9.466	7.091	9.127	11.891	10.557	13.726

Table 13 showed the LCOE of the CAES system without ORC and the CAES system integrated with the ORC associated with different power sources. From the results, if the charging electricity is free, LCOE of the CAES system without the ORC is only 5.247 cents/kWh which is cheaper than that of the integrated system using working fluid, because it is uneconomical to recover waste heat during charging operation of the CAES system when electricity is free. When adopting off-peak time commercial electricity for energy management strategy, the LCOE of the CAES system is still cheaper than residential electricity price (12.75 cents/kWh [72]) and the CAES system integrated with the ORC running in the summer is more economical than the CAES system without the ORC. When the CAES system is supplied with expensive renewable energy, it is evident that LCOE of the CAES system integrated with the ORC is much cheaper than renewable energy except from onshore wind power, and the LCOE of the CAES system integrated with ORC associated with renewable energy is cheaper than that of the CAES system without ORC. The results for solar PV power and offshore wind power cases show the LCOE from the CAES system with the ORC is even lower than power price supplied directly by solar PV and offshore wind power plant. This indicates one important benefit of the CAES system with the ORC, which is that the total amounts of electricity generated from discharging process of the CAES system is almost double with the input rate of electricity during the charging process. The excess part actually is generated by combusting cheap fossil fuel such as natural gas. In this way, integrating the CAES system with the ORC could decrease the expensive prices of electricity from renewable energy such as offshore wind farm and solar power plant.

#### 5.2.4 Comparative LCOEs of power generation technologies



\* R123 is applied as working fluid in CAES system integrated with ORC

Fig. 9 Comparative LCOEs for different power generation technologies

Fig. 9 illustrates comparison of LCOEs of different types of power generation technologies. The CAES system integrated with the ORC associated with different power sources can provide price of electricity that could be competitive with wind power, hydropower and nuclear power, even also some conventional coal power [70,71]. The CAES system integrated with the ORC is capable of solving intermittence of renewable energy and system level needs (such as off-peak oversupply, peak power generation, balancing supply-demand), its functions could have more potential value than reasonable LCOEs [52].

Additionally, the integrated system of the CAES system with the ORC has significant environmental benefits in reduction of carbon emissions. The simulation results showed that the CO<sub>2</sub> emission of this integrated system is 0.1337 kg/kWh. Compare with other power plants, the CO<sub>2</sub> emission from brown coal-fired and hard coal-fired power plants are 1.183 kg/kWh and 1.142 kg/kWh respectively, and that from Natural gas power plants is 0.572 kg/kWh [73]. Hence, the integrated system can release much less CO<sub>2</sub> emission than other power plants.

## 6. Conclusions

In this study, the steady state process model of the proposed CAES system integrated with the ORC was developed in Aspen Plus® with input parameters based on industrial operation considerations. All relative errors of validated models show good agreement and most of them are less than 1%. Technical and economic evaluation were carried out for the effects of different work fluids in the ORC. The LCOE of the integrated system when associated with different power sources was evaluated. The LCOEs were compared with the electricity price from different types of power generation technologies. The main conclusions are summarized as follows:

- The power output and operating temperature of working fluids increase with the operating pressure, the ORC performance is also improved.
- The round-trip efficiency of the CAES system integrated with the ORC has been improved approximately by 3.32-3.95% with different working fluids in the ORC when compared with the CAES system without the ORC.
- R123 as the ORC working fluid has the best performance and the lowest LCOE. The reason is that R123 with a lower EIP. Hence, R123 as working fluid has lower capital cost which leads to a lower LCOE.
- With free or low price off-peak electricity input for the charging process, the LCOE for CAES plant is lower than the residence electricity price. The integrated system of the CAES system with the ORC further decreases the LCOE. That could be effective solution for flexible operating for residence power supply.
- When the offshore wind farm or solar power plants are integrated with the integrated system, their LCOEs could decrease which leads to a lower electricity sale price.

In summary, the CAES system integrated with the ORC as an energy storage technology will not only address the intermittent issue but also could decrease the electricity price for renewable energy to improve their overall economic competitiveness.

## References

- [1] Skea J, Nishioka S. Policies and practices for a low-carbon society. *Climate Policy* 2008;8:S5–16.
- [2] Luo X, Wang J, Dooner M, Clarke J. Overview of current development in electrical energy storage technologies and the application potential in power system operation. *Applied Energy* 2015;137:511–36. doi:10.1016/j.apenergy.2014.09.081.
- [3] Liu X, Chen J, Luo X, Wang M, Meng H. Study on heat integration of supercritical coal-fired power plant with post-combustion CO<sub>2</sub> capture process through process simulation. *Fuel* 2015;158:625–33. doi:10.1016/j.fuel.2015.06.033.
- [4] Ibrahim H, Ilinca A, Perron J. Energy storage systems—Characteristics and comparisons. *Renewable and Sustainable Energy Reviews* 2008;12:1221–50. doi:10.1016/j.rser.2007.01.023.
- [5] Sundararagavan S, Baker E. Evaluating energy storage technologies for wind power integration. *Solar Energy* 2012;86:2707–17. doi:10.1016/j.solener.2012.06.013.
- [6] Radcliffe J. Energy storage technologies. *Ingenia* 2013:Issue 54: 27-32.
- [7] Chen H, Cong TN, Yang W, Tan C, Li Y, Ding Y. Progress in electrical energy storage system: A critical review. *Progress in Natural Science* 2009;19:291–312. doi:10.1016/j.pnsc.2008.07.014.
- [8] Díaz-González F, Sumper A, Gomis-Bellmunt O, Villafáfila-Robles R. A review of energy storage technologies for wind power applications. *Renewable and Sustainable Energy Reviews* 2012;16:2154–71. doi:10.1016/j.rser.2012.01.029.
- [9] Kousksou T, Bruel P, Jamil A, El Rhafiki T, Zeraouli Y. Energy storage: Applications and challenges. *Solar Energy Materials and Solar Cells* 2014;120:59–80. doi:10.1016/j.solmat.2013.08.015.
- [10] Luo X, Wang J, Dooner M, Clarke J, Krupke C. Overview of Current Development in Compressed Air Energy Storage Technology. *Energy Procedia* 2014;62:603–11. doi:10.1016/j.egypro.2014.12.423.
- [11] Chen H, Tan C, Liu J, Zhang X. *Compressed air energy storage*. INTECH Open Access Publisher; 2013.
- [12] Denholm P, Kulcinski GL. Life cycle energy requirements and greenhouse gas emissions from large scale energy storage systems. *Energy Conversion and Management* 2004;45:2153–72. doi:10.1016/j.enconman.2003.10.014.
- [13] Denholm P, Holloway T. Improved accounting of emissions from utility energy storage system operation. *Environmental Science & Technology* 2005;39:9016–22.
- [14] Budt M, Wolf D, Span R, Yan J. A review on compressed air energy storage: Basic principles, past milestones and recent developments. *Applied Energy* 2016;170:250–68. doi:10.1016/j.apenergy.2016.02.108.
- [15] Bouman EA, Øberg MM, Hertwich EG. Life Cycle assessment of compressed air energy storage (CAES). *LCM* 2013, 2013.
- [16] Crotofino F, Mohmeyer K-U, Scharf R. *Huntorf CAES: More than 20 years of successful operation*. Orlando, Florida, USA 2001.
- [17] Robb D. The CAES for wind. *Renewable Energy Focus* 2011;12:18–9. doi:10.1016/S1755-0084(11)70014-X.
- [18] Aneke M, Wang M. Energy storage technologies and real life applications – A state of the art review. *Applied Energy* 2016;179:350–77. doi:10.1016/j.apenergy.2016.06.097.
- [19] Succar S, Williams RH. *Compressed air energy storage: theory, resources, and applications*

- for wind power. Princeton Environmental Institute Report 2008;8.
- [20] Energy Storage R&D Center CA of S. 10MW advanced compressed air energy storage system 2016. <http://english.iet.cas.cn/Institute/6/> (accessed January 20, 2017).
  - [21] Bullough C, Gatzen C, Jakiel C, Koller M, Nowi A, Zunft S. Advanced adiabatic compressed air energy storage for the integration of wind energy. Proceedings of the European Wind Energy Conference, EWEC, vol. 22, 2004, p. 25.
  - [22] Zunft S, Jakiel C, Koller M, Bullough C. Adiabatic compressed air energy storage for the grid integration of wind power. sixth international workshop on large-scale integration of wind power and transmission networks for offshore windfarms, 2006, p. 26–8.
  - [23] Schulte RH, Critelli Jr N, Holst K, Huff G. Lessons from Iowa: development of a 270 megawatt compressed air energy storage project in Midwest independent system operator. Sandia National Laboratories, Albuquerque 2012.
  - [24] Cleary B, Duffy A, OConnor A, Conlon M, Fthenakis V. Assessing the economic benefits of compressed air energy storage for mitigating wind curtailment. IEEE Transactions on Sustainable Energy 2015;6:1021–8.
  - [25] Zhang C. CFD Simulations and Thermal Design for Application to Compressed Air Energy Storage 2015.
  - [26] Zhang C, Yan B, Wieberdink J, Li PY, Van de Ven JD, Loth E, et al. Thermal analysis of a compressor for application to compressed air energy storage. Applied Thermal Engineering 2014;73:1402–11.
  - [27] Iian Yin J, Kim Y-T, Lee Y-H. A hybrid energy storage system using pump compressed air and micro-hydro turbine. Renewable Energy 2014;65:117–22.
  - [28] Raju M, Khaitan SK. Modeling and simulation of compressed air storage in caverns: a case study of the Huntorf plant. Applied Energy 2012;89:474–81.
  - [29] Liu W, Liu L, Zhou L, Huang J, Zhang Y, Xu G, et al. Analysis and optimization of a compressed air energy storage—combined cycle system. Entropy 2014;16:3103–20.
  - [30] Nease J, Adams TA. Systems for peaking power with 100% CO<sub>2</sub> capture by integration of solid oxide fuel cells with compressed air energy storage. Journal of Power Sources 2013;228:281–93.
  - [31] Sun H, Luo X, Wang J. Feasibility study of a hybrid wind turbine system—Integration with compressed air energy storage. Applied Energy 2015;137:617–28.
  - [32] Arsie I, Marano V, Nappi G, Rizzo G. A model of a hybrid power plant with wind turbines and compressed air energy storage. ASME Power Conference, 2005, p. 987–1000.
  - [33] Hartmann N, Vöhringer O, Kruck C, Eltrop L. Simulation and analysis of different adiabatic compressed air energy storage plant configurations. Applied Energy 2012;93:541–8.
  - [34] Quoilin S, Broek M Van Den, Declaye S, Dewallef P, Lemort V. Techno-economic survey of Organic Rankine Cycle (ORC) systems. Renewable and Sustainable Energy Reviews 2013;22:168–86. doi:10.1016/j.rser.2013.01.028.
  - [35] Martínez M, Molina MG, Mercado PE. Dynamic performance of compressed air energy storage (CAES) plant for applications in power systems. Transmission and Distribution Conference and Exposition: Latin America (T&D-LA), 2010 IEEE/PES, IEEE; 2010, p. 496–503.
  - [36] Vélez F, Segovia JJ, Martín MC, Antolín G, Chejne F, Quijano A. A technical, economical and market review of organic Rankine cycles for the conversion of low-grade heat for power generation. Renewable and Sustainable Energy Reviews 2012;16:4175–89. doi:10.1016/j.rser.2012.03.022.
  - [37] Liu B-T, Chien K-H, Wang C-C. Effect of working fluids on organic Rankine cycle for waste

- heat recovery. *Energy* 2004;29:1207–17. doi:10.1016/j.energy.2004.01.004.
- [38] Bronicki LY, Elovic A, Rettger P. Experience with organic Rankine cycles in heat recovery power plants, American Power Conference, Chicago, IL (United States); 1996.
- [39] Kutscher C. Small-scale geothermal power plant field verification projects. *TRANSACTIONS-GEOTHERMAL RESOURCES COUNCIL* 2001:577–80.
- [40] Desai NB, Bandyopadhyay S. Thermo-economic comparisons between solar steam Rankine and organic Rankine cycles. *Applied Thermal Engineering* 2016;105:862–75. doi:10.1016/j.applthermaleng.2016.04.055.
- [41] Liu C, He C, Gao H, Xie H, Li Y, Wu S, et al. The environmental impact of organic Rankine cycle for waste heat recovery through life-cycle assessment. *Energy* 2013;56:144–54.
- [42] Tchanche BF, Lambrinos G, Frangoudakis A, Papadakis G. Low-grade heat conversion into power using organic Rankine cycles – A review of various applications. *Renewable and Sustainable Energy Reviews* 2011;15:3963–79. doi:10.1016/j.rser.2011.07.024.
- [43] Wang J, Yan Z, Wang M, Ma S, Dai Y. Thermodynamic analysis and optimization of an (organic Rankine cycle) ORC using low grade heat source. *Energy* 2013;49:356–65. doi:10.1016/j.energy.2012.11.009.
- [44] Wang M, Wang J, Zhao Y, Zhao P, Dai Y. Thermodynamic analysis and optimization of a solar-driven regenerative organic Rankine cycle (ORC) based on flat-plate solar collectors. *Applied Thermal Engineering* 2013;50:816–25. doi:10.1016/j.applthermaleng.2012.08.013.
- [45] Dai Y, Wang J, Gao L. Parametric optimization and comparative study of organic Rankine cycle (ORC) for low grade waste heat recovery. *Energy Conversion and Management* 2009;50:576–82. doi:10.1016/j.enconman.2008.10.018.
- [46] Freeman J, Hellgardt K, Markides CN. An assessment of solar-powered organic Rankine cycle systems for combined heating and power in UK domestic applications. *Applied Energy* 2015;138:605–20. doi:10.1016/j.apenergy.2014.10.035.
- [47] Chen H, Goswami DY, Stefanakos EK. A review of thermodynamic cycles and working fluids for the conversion of low-grade heat. *Renewable and Sustainable Energy Reviews* 2010;14:3059–67. doi:10.1016/j.rser.2010.07.006.
- [48] Pezzuolo A, Benato A, Stoppato A, Mirandola A. The ORC-PD: A versatile tool for fluid selection and Organic Rankine Cycle unit design. *Energy* 2016;102:605–20. doi:10.1016/j.energy.2016.02.128.
- [49] Butcher di C. L'utilizzo su larga scala dell'energia rinnovabile potrebbe dipendere dalla capacità di immagazzinare l'elettricità 2010. <https://lucaniaelettrica.wordpress.com/2010/05/11/immagazzinare-le-energie-rinnovabili/> (accessed June 7, 2017).
- [50] Elmegaard B, Brix W. Efficiency of compressed air energy storage. 24th International Conference on Efficiency, Cost, Optimization, Simulation and Environmental Impact of Energy Systems, 2011.
- [51] Aneke M, Agnew B, Underwood C. Performance analysis of the Chena binary geothermal power plant. *Applied Thermal Engineering* 2011;31:1825–32. doi:10.1016/j.applthermaleng.2011.02.028.
- [52] McGrail BP, Cabe J, Davidson C, Knudsen F, Bacon D, Bearden M, et al. Technoeconomic Performance Evaluation of Compressed Air Energy Storage in the Pacific Northwest. 2013.
- [53] Luo X. Process modelling, simulation and optimisation of natural gas combined cycle power plant integrated with carbon capture, compression and transport 2016.
- [54] Canepa R, Wang M, Biliyok C, Satta A. Thermodynamic analysis of combined cycle gas

- turbine power plant with post-combustion CO<sub>2</sub> capture and exhaust gas recirculation. Proceedings of the Institution of Mechanical Engineers, Part E: Journal of Process Mechanical Engineering 2013;227:89–105.
- [55] Zhao P, Wang J, Dai Y. Thermodynamic analysis of an integrated energy system based on compressed air energy storage (CAES) system and Kalina cycle. Energy Conversion and Management 2015;98:161–72. doi:10.1016/j.enconman.2015.03.094.
- [56] Bejan A, Tsatsaronis G. Thermal design and optimization. John Wiley & Sons; 1996.
- [57] Hoffeins H. Huntorf air storage gas turbine power plant. Energy Supply, Brown Boveri Publication DGK 1994;90:202.
- [58] Kaiser F. Steady State Analyse of existing Compressed Air Energy Storage Plants. Power and Energy Student Summit (PESS) 2015, January 13th-14th, Dortmund Germany 2015.
- [59] R134a. Gases, Industrial UK n.d. <http://www.boconline.co.uk/en/products-and-supply/refrigerant-gases/hfcs/r134a/index.html> (accessed January 10, 2017).
- [60] Cen K, Chi Y, Yan J. Challenges of power engineering and environment: proceedings of the International Conference on Power Engineering 2007. Springer Science & Business Media; 2009.
- [61] British Refrigeration Association. Guide to Good Commercial Refrigeration Practice Part 2 System Design and Component Selection. 2009.
- [62] Tartière T, Obert B, Sanchez L. thermo-economic optimization of subcritical and transcritical ORC systems. ASME ORC 2013—International seminar on ORC power systems, 2013.
- [63] Air Conditioning and Refrigeration Guide. Water cooled chiller n.d. <http://www.air-conditioning-and-refrigeration-guide.com/water-cooled-chiller.html> (accessed March 20, 2017).
- [64] El-Wakil MM. Powerplant technology. Tata McGraw-Hill Education; 1984.
- [65] Desai NB, Bandyopadhyay S. Process integration of organic Rankine cycle. Energy 2009;34:1674–86. doi:10.1016/j.energy.2009.04.037.
- [66] Luo X, Wang M, Oko E, Okezue C. Simulation-based techno-economic evaluation for optimal design of CO<sub>2</sub> transport pipeline network. Applied Energy 2014;132:610–20. doi:10.1016/j.apenergy.2014.07.063.
- [67] Luo X, Wang M. Study of solvent-based carbon capture for cargo ships through process modelling and simulation. Applied Energy 2017;195:402–13.
- [68] Administration U. EI. NATURAL GAS 2016. <https://www.eia.gov/dnav/ng/hist/n3035us3M.htm> (accessed January 20, 2017).
- [69] Pacific Power. Time of Use Hours & Pricing 2017. <https://www.pacificpower.net/ya/po/otou/ooh.html> (accessed January 20, 2017).
- [70] OpenEI. Transparent Cost Database 2015. <http://en.openei.org/apps/TCDB/#blank> (accessed January 10, 2016).
- [71] LAZARD. LAZARD'S LEVELIZED COST OF ENERGY ANALYSIS — VERSION 8.0. 2014.
- [72] U.S. Energy Information Administration. Electric Power Monthly 2016. [https://www.eia.gov/electricity/monthly/epm\\_table\\_grapher.cfm?t=epmt\\_5\\_6\\_a](https://www.eia.gov/electricity/monthly/epm_table_grapher.cfm?t=epmt_5_6_a) (accessed January 20, 2017).
- [73] WINGAS. Natural gas is the most climate-friendly fossil fuel in electricity production n.d. [https://www.wingas.com/fileadmin/Wingas/WINGAS-Studien/Energieversorgung\\_und\\_Energiewende\\_en.pdf](https://www.wingas.com/fileadmin/Wingas/WINGAS-Studien/Energieversorgung_und_Energiewende_en.pdf) (accessed July 9, 2017).

